

# LA-UR-13-20429

Approved for public release; distribution is unlimited.

Title: Fission Matrix Capability for MCNP, Part I - Theory

Author(s): Brown, Forrest B.  
Carney, Sean E.  
Kiedrowski, Brian C.  
Martin, William R.

Intended for: Mathematics & Computation 2013, 2013-05-05/2013-05-09 (Sun Valley, Idaho, United States)  
MCNP documentation  
Web



**Disclaimer:**

Los Alamos National Laboratory, an affirmative action/equal opportunity employer, is operated by the Los Alamos National Security, LLC for the National Nuclear Security Administration of the U.S. Department of Energy under contract DE-AC52-06NA25396. By approving this article, the publisher recognizes that the U.S. Government retains nonexclusive, royalty-free license to publish or reproduce the published form of this contribution, or to allow others to do so, for U.S. Government purposes. Los Alamos National Laboratory requests that the publisher identify this article as work performed under the auspices of the U.S. Department of Energy. Los Alamos National Laboratory strongly supports academic freedom and a researcher's right to publish; as an institution, however, the Laboratory does not endorse the viewpoint of a publication or guarantee its technical correctness.

## **FISSION MATRIX CAPABILITY FOR MCNP, PART I - THEORY**

**F.B. Brown<sup>1</sup>, S.E. Carney<sup>2</sup>, B.C. Kiedrowski<sup>1</sup>, W.R. Martin<sup>2</sup>**

<sup>1</sup> Los Alamos National Laboratory, Monte Carlo Codes Group  
PO Box 1663, MS A143, Los Alamos, NM 87545, USA  
fbrown@lanl.gov; bckiedro@lanl.gov

<sup>2</sup> University of Michigan, NERS Department  
2355 Bonisteel Boulevard, Ann Arbor, MI 48109, USA  
seanec@umich.edu; wrm@umich.edu

### **ABSTRACT**

The theory underlying the fission matrix method is derived using a rigorous Green's function approach. The method is then used to investigate fundamental properties of the transport equation for a continuous-energy physics treatment. We provide evidence that an infinite set of discrete, real eigenvalues and eigenfunctions exist for the continuous-energy problem, and that the eigenvalue spectrum converges smoothly as the spatial mesh for the fission matrix is refined. We also derive equations for the adjoint solution. We show that if the mesh is sufficiently refined so that both forward and adjoint solutions are valid, then the adjoint fission matrix is identical to the transpose of the forward matrix. While the energy-dependent transport equation is strictly biorthogonal, we provide surprising results that the forward modes are very nearly self-adjoint for a variety of continuous-energy problems. A companion paper (Part II – Applications) describes the initial experience and results from implementing this fission matrix capability into the MCNP Monte Carlo code.

*Key Words:* Monte Carlo, neutron transport, eigenvalues, adjoint

### **1. INTRODUCTION**

Continuous-energy Monte Carlo codes such as MCNP [1] simulate neutron behavior using the best available nuclear data, accurate physics models, and detailed geometry models. Reactor criticality calculations for  $k_{eff}$  and the power distribution are carried out iteratively, using the power method, where batches of neutrons are simulated for a single generation. The first-generation fission neutrons produced in a batch become the starting neutron sites for the next batch. A suitable number of “inactive” initial batches are required to converge to the fundamental mode eigenvalue and eigenfunction, and then succeeding iterations with “active” batches are used to accumulate Monte Carlo tallies for estimating desired reaction rate distributions.

Most Monte Carlo codes perform the power iteration without acceleration and can sometimes exhibit very slow convergence. Statistical noise for batch results precludes the use of common outer iteration acceleration methods (e.g., Chebyshev). Also, since production Monte Carlo codes restrict neutron statistical weights to be non-negative, higher eigenmodes cannot be evaluated directly from the Monte Carlo neutron simulation.

The fission matrix approach was proposed in the earliest works on Monte Carlo criticality calculations [2-4] and has been tried by many researchers over the years. The present work provides a rigorous derivation of the forward and adjoint forms of the fission matrix treatment for k-eigenvalue problems. The method is then used to investigate fundamental properties of the transport equation for a continuous-energy physics treatment, for both forward and adjoint modes. A companion paper (Part II – Applications [5]) describes the initial experience and results from implementing this fission matrix capability into the MCNP Monte Carlo code.

## 2. THEORETICAL BASIS OF THE FISSION MATRIX

In the following sections, we first provide a derivation of the k-effective form of the integral transport equations for the forward and adjoint fission neutron sources for continuous-energy problems using a rigorous Green's function approach (Sections 2.1 – 2.3). The integral equations are then integrated over spatial regions to provide an exact prescription for the fission matrix elements and resulting equations for the regionwise sources (Sections 2.4 – 2.5). The solution to the fission matrix equations is shown to be exact if the within-region weighting functions are known, or in the limit of vanishingly small region size. Subsequent sections examine properties of the eigenvalue spectrum, including convergence with refinement in the region size, the question of strictly real eigenvalues, and the effect of Monte Carlo statistical noise.

### 2.1 Integral Equation for the Neutron Source

The k-eigenvalue form of the neutron transport equation is

$$\mathbf{M} \cdot \Psi(\vec{r}, E, \hat{\Omega}) = \frac{1}{k} \cdot \frac{\chi(E)}{4\pi} \cdot \mathbf{S}(\vec{r}), \quad (1)$$

where  $\mathbf{M}$  is the net loss operator defined by

$$\mathbf{M} \cdot \Psi(\vec{r}, E, \hat{\Omega}) = \hat{\Omega} \cdot \nabla \Psi(\vec{r}, E, \hat{\Omega}) + \Sigma_T(\vec{r}, E) \Psi(\vec{r}, E, \hat{\Omega}) - \iint dE' d\hat{\Omega}' \Sigma_S(\vec{r}, E' \rightarrow E, \hat{\Omega}' \rightarrow \hat{\Omega}) \Psi(\vec{r}, E', \hat{\Omega}'), \quad (2)$$

$\mathbf{S}(\vec{r})$  is the fission neutron source, defined by

$$\mathbf{S}(\vec{r}) = \iint dE' d\hat{\Omega}' \nu \Sigma_F(\vec{r}, E') \Psi(\vec{r}, E', \hat{\Omega}'), \quad (3)$$

and  $\chi(E)$  is the emission energy spectrum of fission neutrons. Fission neutron emission is assumed to be isotropic. To simplify the analysis that follows,  $\chi(E)$  is assumed to be independent of the energy of the neutrons causing fission. (See Appendix A for discussion.) All other terms are defined in the usual way.

The Green's function for this problem is defined by the equation

$$\mathbf{M} \cdot \mathbf{G}(\vec{r}_0, E_0, \hat{\Omega}_0 \rightarrow \vec{r}, E, \hat{\Omega}) = \delta(\vec{r} - \vec{r}_0) \cdot \delta(E - E_0) \cdot \delta(\hat{\Omega} - \hat{\Omega}_0), \quad (4)$$

where the “0” subscript denotes an initial point in phase space, and  $\delta$  is the Dirac delta function. Then, based on linearity of the transport equation and the superposition principle, it follows that

$$\Psi(\vec{r}, E, \hat{\Omega}) = \frac{1}{k} \cdot \iiint d\vec{r}_0 dE_0 d\hat{\Omega}_0 \frac{\chi(E_0)}{4\pi} \cdot \mathbf{S}(\vec{r}_0) \cdot \mathbf{G}(\vec{r}_0, E_0, \hat{\Omega}_0 \rightarrow \vec{r}, E, \hat{\Omega}) \quad (5)$$

Eq. (5) is the k-eigenvalue form of Peierls equation. Now multiply Eq. (5) by  $\nu \Sigma_F(\vec{r}, E)$  and integrate over all  $E$  and  $\hat{\Omega}$ :

$$\iint dE d\hat{\Omega} \cdot v \Sigma_F(\bar{r}, E) \Psi(\bar{r}, E, \hat{\Omega}) = \frac{1}{k} \cdot \iint dE d\hat{\Omega} \cdot v \Sigma_F(\bar{r}, E) \iiint d\bar{r}_0 dE_0 d\hat{\Omega}_0 \frac{\chi(E_0)}{4\pi} S(\bar{r}_0) G(\bar{r}_0, E_0, \hat{\Omega}_0 \rightarrow \bar{r}, E, \hat{\Omega}) \quad (6)$$

$$S(\bar{r}) = \frac{1}{k} \cdot \int d\bar{r}_0 \cdot S(\bar{r}_0) \cdot \int \iiint dE d\hat{\Omega} dE_0 d\hat{\Omega}_0 \cdot v \Sigma_F(\bar{r}, E) \cdot \frac{\chi(E_0)}{4\pi} \cdot G(\bar{r}_0, E_0, \hat{\Omega}_0 \rightarrow \bar{r}, E, \hat{\Omega})$$

Introducing the kernel  $H(\bar{r}_0 \rightarrow \bar{r})$  to represent the energy-angle averaged Green's function,

$$H(\bar{r}_0 \rightarrow \bar{r}) = \int \iiint dE d\hat{\Omega} dE_0 d\hat{\Omega}_0 \cdot v \Sigma_F(\bar{r}, E) \cdot \frac{\chi(E_0)}{4\pi} \cdot G(\bar{r}_0, E_0, \hat{\Omega}_0 \rightarrow \bar{r}, E, \hat{\Omega}), \quad (7)$$

substituting Eq. (7) into Eq. (6) results in:

$$S(\bar{r}) = \frac{1}{k} \cdot \int d\bar{r}_0 \cdot S(\bar{r}_0) \cdot H(\bar{r}_0 \rightarrow \bar{r}) \quad (8)$$

Eq. (8) is an integral equation for the neutron source at  $\bar{r}$  expressed in terms of the kernel  $H$ .  $H$  is simply the Green's function integrated over angles and energies, weighted by the initial spectrum and final fission neutron production. While  $H$  is not generally useful for analytic work, it can readily be evaluated by either continuous-energy or multigroup Monte Carlo without any approximation. That is, the Green's function  $G$  is provided directly by the transport simulation in a Monte Carlo code; the energy-angle integration to produce  $H$  in Eq. (7) is simply a tally in the Monte Carlo simulation, binned according to the initial and final spatial positions. It should be noted that no approximations were made in obtaining Eqs. (7) and (8).

## 2.2 Integral Equation for the Adjoint Neutron Source

The k-eigenvalue form of the adjoint neutron transport equation can be written as

$$M^\dagger \cdot \Psi^\dagger(\bar{r}, E, \hat{\Omega}) = \frac{1}{k} \cdot v \Sigma_F(\bar{r}, E) \cdot S^\dagger(\bar{r}), \quad (9)$$

where  $M^\dagger$  is the operator adjoint to  $M$ , defined by

$$M^\dagger \cdot \Psi^\dagger(\bar{r}, E, \hat{\Omega}) = -\hat{\Omega} \cdot \nabla \Psi^\dagger(\bar{r}, E, \hat{\Omega}) + \Sigma_T(\bar{r}, E) \Psi^\dagger(\bar{r}, E, \hat{\Omega}) - \iint dE' d\hat{\Omega}' \Sigma_S(\bar{r}, E \rightarrow E', \hat{\Omega} \rightarrow \hat{\Omega}') \Psi^\dagger(\bar{r}, E', \hat{\Omega}'), \quad (10)$$

$S^\dagger(\bar{r})$  is the adjoint source, defined by

$$S^\dagger(\bar{r}) = \iint dE' d\hat{\Omega}' \frac{\chi(E')}{4\pi} \Psi^\dagger(\bar{r}, E', \hat{\Omega}'), \quad (11)$$

Bell and Glasstone [6] and others have shown that the eigenvalue  $K$  in Eq. (9) is identical to the eigenvalue  $K$  in Eq. (1), hence the analysis below will just use  $K$ , rather than  $K$  and  $K^\dagger$ .

The Green's function for this problem is defined by the equation

$$M^\dagger \cdot G^\dagger(\bar{r}_0, E_0, \hat{\Omega}_0 \rightarrow \bar{r}, E, \hat{\Omega}) = \delta(\bar{r} - \bar{r}_0) \cdot \delta(E - E_0) \cdot \delta(\hat{\Omega} - \hat{\Omega}_0), \quad (12)$$

where the "0" subscript denotes an initial point in phase space, and  $\delta$  is the Dirac delta function. It then follows that

$$\Psi^\dagger(\bar{r}, E, \hat{\Omega}) = \frac{1}{k} \cdot \iiint d\bar{r}_0 dE_0 d\hat{\Omega}_0 v \Sigma_F(\bar{r}_0, E_0) \cdot S^\dagger(\bar{r}_0) \cdot G^\dagger(\bar{r}_0, E_0, \hat{\Omega}_0 \rightarrow \bar{r}, E, \hat{\Omega}) \quad (13)$$

Now multiply Eq. (13) by  $\chi(E)/4\pi$  and integrate over all  $E$  and  $\hat{\Omega}$ :

$$\begin{aligned} \iint dE d\hat{\Omega} \frac{\chi(E)}{4\pi} \Psi^+(\vec{r}, E, \hat{\Omega}) &= \frac{1}{k} \cdot \iint dE d\hat{\Omega} \cdot \frac{\chi(E)}{4\pi} \iiint d\vec{r}_0 dE_0 d\hat{\Omega}_0 \cdot v\Sigma_F(\vec{r}_0, E_0) \cdot S^+(\vec{r}_0) G^+(\vec{r}_0, E_0, \hat{\Omega}_0 \rightarrow \vec{r}, E, \hat{\Omega}) \\ S^+(\vec{r}) &= \frac{1}{k} \cdot \int d\vec{r}_0 \cdot S^+(\vec{r}_0) \cdot \int \iiint dE d\hat{\Omega} dE_0 d\hat{\Omega}_0 \frac{\chi(E)}{4\pi} \cdot v\Sigma_F(\vec{r}_0, E_0) \cdot G^+(\vec{r}_0, E_0, \hat{\Omega}_0 \rightarrow \vec{r}, E, \hat{\Omega}) \end{aligned} \quad (14)$$

Eq. (14) is an integral equation for the adjoint source at  $\vec{r}$ , with the Green's function integrated over angles and energies, weighted by the initial spectrum and final fission neutron production. Introducing the operator  $H^+(\vec{r}_0 \rightarrow \vec{r})$  to represent the averaged Green's function,

$$H^+(\vec{r}_0 \rightarrow \vec{r}) = \int \iiint dE d\hat{\Omega} dE_0 d\hat{\Omega}_0 \frac{\chi(E)}{4\pi} \cdot v\Sigma_F(\vec{r}_0, E_0) \cdot G^+(\vec{r}_0, E_0, \hat{\Omega}_0 \rightarrow \vec{r}, E, \hat{\Omega}), \quad (15)$$

substituting Eq. (15) into Eq. (14) results in:

$$S^+(\vec{r}) = \frac{1}{k} \cdot \int d\vec{r}_0 \cdot S^+(\vec{r}_0) \cdot H^+(\vec{r}_0 \rightarrow \vec{r}) \quad (16)$$

The reciprocity relation between the direct and adjoint Green's function is

$$G^+(\vec{r}_0, E_0, \hat{\Omega}_0 \rightarrow \vec{r}, E, \hat{\Omega}) = G(\vec{r}, E, \hat{\Omega} \rightarrow \vec{r}_0, E_0, \hat{\Omega}_0) \quad (17)$$

Because of the irreversible energy dependence in the neutron slowing down process, neither  $G$  nor  $G^+$  is symmetric in the initial and final arguments, and Eq. (17) is the correct reciprocity relation [6]. Substituting the reciprocity relation into Eq. (15) and comparing with Eq. (7) gives

$$\begin{aligned} H^+(\vec{r}_0 \rightarrow \vec{r}) &= \int \iiint dE d\hat{\Omega} dE_0 d\hat{\Omega}_0 \frac{\chi(E)}{4\pi} \cdot v\Sigma_F(\vec{r}_0, E_0) \cdot G(\vec{r}, E, \hat{\Omega} \rightarrow \vec{r}_0, E_0, \hat{\Omega}_0) \\ &= H(\vec{r} \rightarrow \vec{r}_0) \end{aligned} \quad (18)$$

Eq. (16) then becomes

$$S^+(\vec{r}) = \frac{1}{k} \cdot \int d\vec{r}_0 \cdot S^+(\vec{r}_0) \cdot H(\vec{r} \rightarrow \vec{r}_0) \quad (19)$$

Eq. (19) is an integral equation for the adjoint neutron source at  $\vec{r}$  expressed in terms of the kernel  $H$ . No approximations were made in obtaining Eqs. (18) and (19).

### 2.3 Comments on the Forward and Adjoint Integral Equations for the Neutron Source

The integral equations for the neutron source and adjoint neutron source given by Eqs. (8) and (19) are

$$S(\vec{r}) = \frac{1}{k} \cdot \int d\vec{r}_0 \cdot S(\vec{r}_0) \cdot H(\vec{r}_0 \rightarrow \vec{r}) \quad (20a)$$

$$S^+(\vec{r}) = \frac{1}{k} \cdot \int d\vec{r}_0 \cdot S^+(\vec{r}_0) \cdot H(\vec{r} \rightarrow \vec{r}_0) \quad (20b)$$

$H$  and  $H^+$  are not symmetric in their arguments, but jointly obey the same reciprocity relation as in Eq. (17). That is,

$$\begin{aligned} H(\vec{r}_0 \rightarrow \vec{r}) &\neq H(\vec{r} \rightarrow \vec{r}_0) \\ H^+(\vec{r}_0 \rightarrow \vec{r}) &\neq H^+(\vec{r} \rightarrow \vec{r}_0) \\ H^+(\vec{r}_0 \rightarrow \vec{r}) &= H(\vec{r} \rightarrow \vec{r}_0) \end{aligned} \quad (21)$$

The fundamental mode eigenvalues and eigenfunctions of Eqs. (20) have been proven to exist, even for the continuous-energy form of the transport equation [7]. The fundamental mode eigenvalue is real, and the fundamental mode eigenfunction is non-negative.

For the 1-speed integral transport equation for the scalar flux derived from Eq. (1) assuming isotropic scattering, it has been proven [8] that all of the higher modes exist, with discrete real eigenvalues and real eigenfunctions. The 1-speed integral equation for the scalar flux is self-adjoint due to the symmetry of the kernel in the integral equations. (In the notation used here, the kernel  $H(\vec{r}_0 \rightarrow \vec{r})$  is equal to  $H(\vec{r} \rightarrow \vec{r}_0)$  for a 1-speed treatment; an integral operator with a symmetric kernel has an infinite set of discrete real eigenvalues and associated real eigenfunctions.) This proof was later extended to include anisotropic scattering [9].

For the multigroup transport equation and the continuous-energy transport equation, it is conventional practice to assume that higher modes exist, with real eigenvalues and eigenfunctions, even though that has not been proven. (This assumption will be confirmed below, using the fission matrix and continuous-energy Monte Carlo for determining the source eigenfunctions.)

Letting  $K_n$  denote the  $n$ -th eigenvalue of Eqs. (20),  $S_n(\vec{r})$  the  $n$ -th eigenfunction, and  $S_n^+(\vec{r})$  the  $n$ -th adjoint eigenfunction, with  $n=0$  denoting the fundamental mode and  $n>0$  the higher modes,

$$\begin{aligned} S_n(\vec{r}) &= \frac{1}{K_n} \int d\vec{r}_0 \cdot S_n(\vec{r}_0) \cdot H(\vec{r}_0 \rightarrow \vec{r}) \\ S_n^+(\vec{r}) &= \frac{1}{K_n} \int d\vec{r}_0 \cdot S_n^+(\vec{r}_0) \cdot H(\vec{r} \rightarrow \vec{r}_0) \end{aligned} \quad (22)$$

The orthogonality relations for Eqs. (21) are

$$(K_p - K_q) \cdot \int d\vec{r} \cdot S_p(\vec{r}) \cdot S_q^+(\vec{r}) = 0 \quad (23)$$

It should be noted that, based upon the transport equation and the rigorous treatment above, that there is no basis for assuming that the forward eigenfunctions alone form an orthogonal basis set (i.e., are self-adjoint). Indeed they should not, because the energy-angle averaged Green's function  $H$  is not a symmetric function of its arguments.

### 3. FORWARD AND ADJOINT FISSION MATRIX EQUATIONS

#### 3.1 Forward Fission Matrix Equations

If the physical problem is segmented into  $N$  spatial regions, and Eqs. (7) and (8) are then integrated over the volumes of each initial region  $J$ , with  $\vec{r}_0 \in V_J$ , and final region  $I$ , with  $\vec{r} \in V_I$ , then the following equations are obtained:

$$S_I = \frac{1}{K} \cdot \sum_{J=1}^N F_{I,J} \cdot S_J \quad (24)$$

where

$$F_{I,J} = \int_{\vec{r} \in V_I} d\vec{r} \int_{\vec{r}_0 \in V_J} d\vec{r}_0 \frac{S(\vec{r}_0)}{S_J} \cdot H(\vec{r}_0 \rightarrow \vec{r}), \quad S_J = \int_{\vec{r} \in V_J} S(\vec{r}') d\vec{r}' \quad (25)$$

The matrix element  $F_{I,J}$  is equal to the number of fission neutrons born in region  $I$  due to one average fission neutron starting in region  $J$ . The matrix  $\bar{F}$  is called the *fission matrix*. The fundamental mode eigenvalue of this matrix is formally identical to the eigenvalue  $K$  in Eq. (1), and the fundamental mode eigenvector is the regionwise fission neutron source distribution. In matrix-vector form, Eq. (24) is

$$\bar{S} = \frac{1}{K} \cdot \bar{F} \cdot \bar{S} \quad (26)$$

where  $\vec{S}$  is a vector of length  $N$  giving the single-generation production of neutrons in each region from fission, and  $\vec{F}$  is a full matrix of size  $N \times N$ .  $K$  is formally identical to  $k_{eff}$ , the eigenvalue of the system.

Eqs. (24-25) and (26) are exact; no approximations were made in formulating them. The interpretation of the  $S_I$  terms, however, requires some discussion. Each  $S_I$  term is the single-generation production of fission neutrons in region  $V_I$ . If the regions  $V_I$  are small enough, then  $S_I / V_I$  represents a discrete approximation to the actual source  $S(\vec{r})$  from Eq. (3). The notion of “small enough” will be discussed below.

### 3.2 Adjoint Fission matrix Equations

If the physical problem is segmented into  $N$  spatial regions, and Eqs. (18) and (19) are then integrated over the volumes of each initial region  $J$ , with  $\vec{r}_0 \in V_J$ , and final region  $I$ , with  $\vec{r} \in V_I$ , then the following equations are obtained:

$$S_I^\dagger = \frac{1}{K} \cdot \sum_{J=1}^N F_{I,J}^\dagger \cdot S_J^\dagger \quad (27)$$

where

$$F_{I,J}^\dagger = \int_{\vec{r} \in V_I} d\vec{r} \int_{\vec{r}_0 \in V_J} d\vec{r}_0 \cdot \frac{S^\dagger(\vec{r}_0)}{S_J^\dagger} \cdot H(\vec{r} \rightarrow \vec{r}_0), \quad S_J^\dagger = \int_{\vec{r}' \in V_J} S^\dagger(\vec{r}') d\vec{r}' \quad (28)$$

In matrix-vector form, Eq. (27) is

$$\vec{S}^\dagger = \frac{1}{K} \cdot \vec{F}^\dagger \cdot \vec{S}^\dagger \quad (29)$$

The components of the adjoint vector  $\vec{S}^\dagger$  are the importances of the fission neutrons born in each region  $I$  of the problem. Equations (27)-(29) are the adjoint form of Eqs (24)-(26). The eigenvalue  $K$  of these equations is formally identical to that in Eq. (1) and Eq. (9).

### 3.3 Relationship Between the Forward and adjoint Fission Matrix

To compare the matrices  $\vec{F}$  and  $\vec{F}^\dagger$ , it is instructive to examine the fission matrix elements for the direct and adjoint matrices for a particular  $(I,J)$  entry:

$$F_{I,J} = \int_{\vec{r} \in V_I} d\vec{r} \int_{\vec{r}_0 \in V_J} d\vec{r}_0 \cdot \frac{S(\vec{r}_0)}{S_J} \cdot \int \int \int dE d\hat{\Omega} dE_0 d\hat{\Omega}_0 \cdot v \Sigma_F(\vec{r}, E) \cdot \frac{\chi(E_0)}{4\pi} \cdot G(\vec{r}_0, E_0, \hat{\Omega}_0 \rightarrow \vec{r}, E, \hat{\Omega}) \quad (32a)$$

$$F_{I,J}^\dagger = \int_{\vec{r} \in V_I} d\vec{r} \int_{\vec{r}_0 \in V_J} d\vec{r}_0 \cdot \frac{S^\dagger(\vec{r}_0)}{S_J^\dagger} \cdot \int \int \int dE d\hat{\Omega} dE_0 d\hat{\Omega}_0 \cdot v \Sigma_F(\vec{r}_0, E_0) \cdot \frac{\chi(E)}{4\pi} \cdot G(\vec{r}, E, \hat{\Omega} \rightarrow \vec{r}_0, E_0, \hat{\Omega}_0) \quad (32b)$$

To clarify the relation between  $\vec{F}$  and  $\vec{F}^\dagger$ , it is helpful to reverse the subscripts and formally interchange the integration variables in Eq. (32b), and to then compare  $F_{I,J}$  with  $F_{J,I}^\dagger$ :

$$F_{I,J} = \int_{\vec{r} \in V_I} d\vec{r} \int_{\vec{r}_0 \in V_J} d\vec{r}_0 \cdot \frac{S(\vec{r}_0)}{S_J} \cdot \int \int \int dE d\hat{\Omega} dE_0 d\hat{\Omega}_0 \cdot v \Sigma_F(\vec{r}, E) \cdot \frac{\chi(E_0)}{4\pi} \cdot G(\vec{r}_0, E_0, \hat{\Omega}_0 \rightarrow \vec{r}, E, \hat{\Omega}) \quad (33a)$$

$$F_{J,I}^\dagger = \int_{\vec{r}_0 \in V_J} d\vec{r}_0 \int_{\vec{r} \in V_I} d\vec{r} \cdot \frac{S^\dagger(\vec{r})}{S_I^\dagger} \cdot \int \int \int dE d\hat{\Omega} dE_0 d\hat{\Omega}_0 \cdot v \Sigma_F(\vec{r}, E) \cdot \frac{\chi(E_0)}{4\pi} \cdot G(\vec{r}_0, E_0, \hat{\Omega}_0 \rightarrow \vec{r}, E, \hat{\Omega}) \quad (33b)$$

It can be seen that while the Green's functions and physical data in the energy-angle integrations are identical, the spatial weighting functions differ in Eqs. (33a) and (33b). For Eq. (33a) the spatial weighting function is  $S(\mathbf{r}_0)/S_J$ , while for Eq. (33b) the spatial weighting function is  $S^T(\mathbf{r})/S_I$ . If the spatial mesh used for the fission matrix is fine enough so that

$$\frac{S^+(\bar{\mathbf{r}})}{S_I^+/V_I} \approx 1 \quad \text{for } \bar{\mathbf{r}} \in V_I \quad \text{and} \quad \frac{S(\bar{\mathbf{r}}_0)}{S_J/V_J} \approx 1 \quad \text{for } \bar{\mathbf{r}}_0 \in V_J \quad (34)$$

then Eqs. (33a) and (33b) become identical, and  $F_{i,j} = F_{j,i}^+$ . That is, in the limit of a fine enough spatial mesh, the adjoint fission matrix is equal to the transpose of the (direct) fission matrix,

$$\bar{\mathbf{F}}^+ = \bar{\mathbf{F}}^T, \quad (35)$$

so that the fission matrix equations are consistent with the continuous formulation given by Eq. (18).

### 3.4 Monte Carlo Estimation of the Fission Matrix

As noted in Section 2.1, the fission matrix elements defined rigorously by Eqs. (33) may be estimated by continuous-energy Monte Carlo methods. The Green's function  $G$  is provided directly by the transport simulation in a Monte Carlo code; the energy-angle integration is simply a tally in the Monte Carlo simulation, binned according to the initial and final region indices. If a coarse mesh is used to define the spatial regions for tallying Eqs. (33), then the tallies cannot be made until after the fission source distribution has converged, since the spatial weighting functions correspond to the stationary source distribution. However, if a fine enough mesh is used such that Eq. (34) is valid, then Eqs. (33) become independent of the spatial weighting functions, and valid tallies can be made even before the source distribution converges. In the next Section and in Part II [5], studies of the convergence of fission matrix results with mesh refinement are used to demonstrate the validity of this approach.

While Part II provides details of the MCNP implementation of the fission matrix method, a short summary is provided here. During a standard  $k$ -effective calculation, at the end of each cycle the  $F_{I,J}$  estimators are updated by tallying the fission neutron weight using the starting and ending mesh region numbers for each point in fission bank. These tallies are non-intrusive, performed only at the end of a cycle, not during the within-cycle random walks, and consume only a trivial amount of cpu time. If the mesh is fine enough that Eq. (34) is valid, the tallies may be accumulated over cycles even during the inactive cycles, prior to convergence of the fission source distribution. At any desired cycle, the  $F_{I,J}$  tallies may be normalized by dividing by the total accumulated source in the starting regions (i.e.,  $J$  index) to form the normalized fission matrix. Then the eigenvalues and eigenvectors of the fission matrix may be found by simple power iteration. (If higher modes are desired, as discussed in the next Section, then Hotelling deflation or direct solvers may be also be used.)

## 4. FISSION MATRIX EIGENMODES AND EIGENVALUE SPECTRUM

### 4.1 Basis for Higher Eigenmode Analysis Using the Fission Matrix

Eqs. (8) and (19) are specific to the fundamental modes of the forward and adjoint  $k$ -eigenvalue transport equation for continuous-energy problems. Higher modes have always been assumed to exist for Eqs. (8) and (19). For the discretized, region-integrated Eqs. (26) and (29) for the fission matrix approach, higher eigenmodes can be determined according to:

$$\begin{aligned}
\bar{S}_n &= \frac{1}{k_n} \cdot \bar{F} \cdot \bar{S}_n, \\
\bar{S}_n^\dagger &= \frac{1}{k_n} \cdot \bar{F}^\top \cdot \bar{S}_n^\dagger, \quad n = 0, 1, \dots, N \\
k_0 &> |k_1| > |k_2| > \dots > |k_N|
\end{aligned} \tag{36}$$

where the subscript  $n$  refers to the mode, with  $n=0$  the fundamental mode. In Eqs. (36), the adjoint fission matrix has been replaced by the transpose of the direct fission matrix, according to the discussion regarding Eq. (35). For a problem with  $N$  regions in the mesh for the fission matrix,  $\bar{F}$  is an  $N \times N$  matrix with  $N$  discrete eigenvalues. Because  $\bar{F}$  is a nonsymmetric matrix, the eigenvalues and eigenvectors may be complex, although the fundamental mode must be strictly real.

Because the transport equation is biorthogonal, different eigenvectors  $\bar{S}_p$  and  $\bar{S}_q$  (and also  $\bar{S}_p^\dagger$  and  $\bar{S}_q^\dagger$ ) need not be orthogonal to each other. The forward and adjoint eigenvectors,  $\bar{S}_p$  and  $\bar{S}_q^\dagger$ , however, are orthogonal:

$$(k_p - k_q) \cdot (\bar{S}_p \cdot \bar{S}_q^\dagger) = 0 \tag{37}$$

It should be noted that the adjoint eigenvectors  $\bar{S}_q^\dagger$  can be interpreted as the *left* eigenvectors of the matrix  $\bar{F}$ , while the forward eigenvectors  $\bar{S}_p$  are the *right* eigenvectors of the matrix  $\bar{F}$ . It is a mathematical identity that the left and right eigenvectors of a matrix are orthogonal.

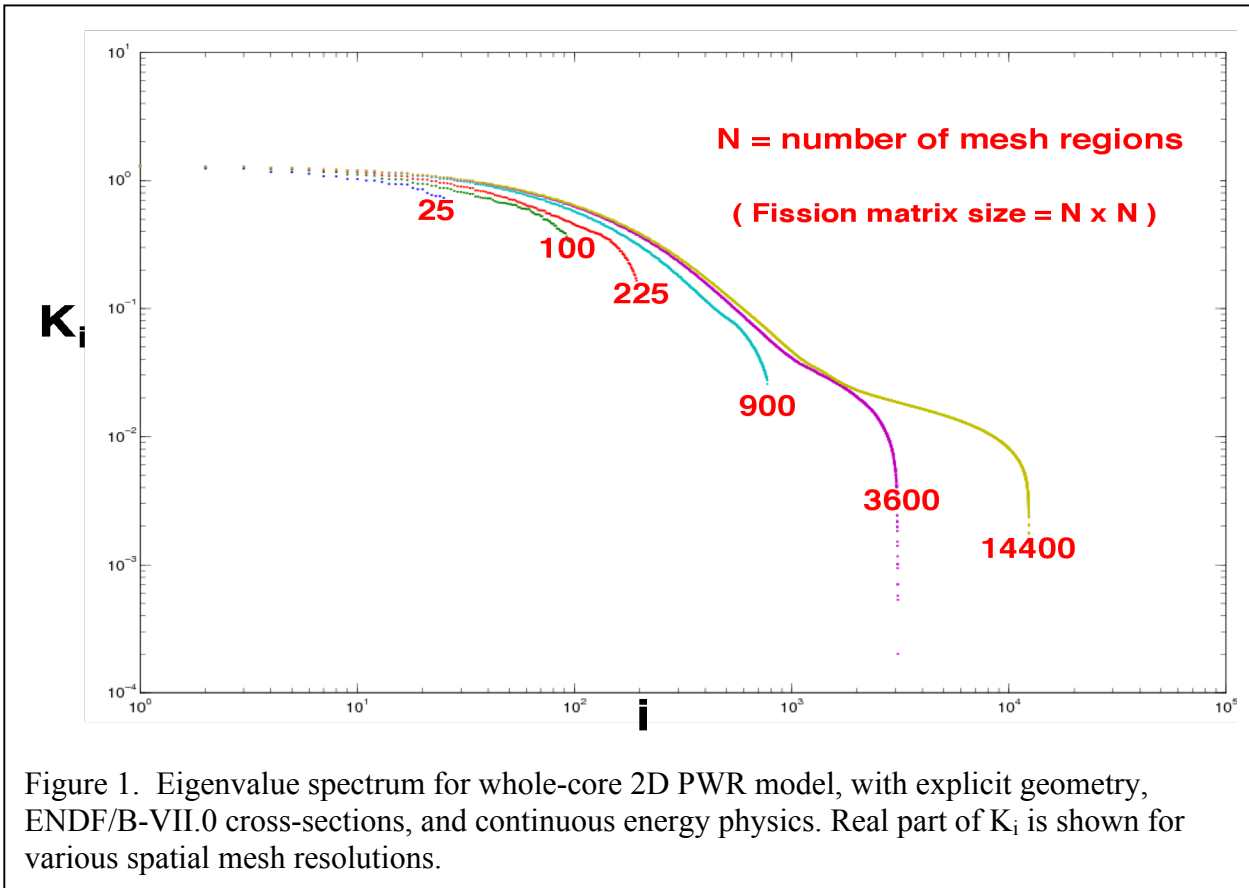
#### 4.2 Spectrum Convergence with Mesh Refinement

When the fission matrix is estimated during a continuous-energy Monte Carlo  $k$ -effective calculation, the  $N$  eigenvalues of the  $N \times N$  fission matrix may be determined, where  $N$  is the number of regions in the spatial mesh used for tallying the fission matrix. If the calculation is repeated using finer mesh resolution, i.e., higher  $N$ , then convergence of the eigenvalue spectrum is observed. That is, for some value of  $N$ , the eigenvalue spectrum appears to have converged to its limiting distribution such that further mesh refinement does not alter the spectrum. Convergence of the eigenvalue spectrum provides direct evidence that the spatial mesh resolution is fine enough that Eq. (34) is valid.

Figure 1 provides an example of a mesh refinement study for the eigenvalue spectrum for a whole-core 2D PWR model, with explicit geometry, ENDF/B-VII.0 cross-sections, and continuous energy physics [5,11,12]. As the mesh is refined (larger  $N$ , smaller region size), it is seen that the spectrum for the first few 100 or 1000 eigenvalues converges.

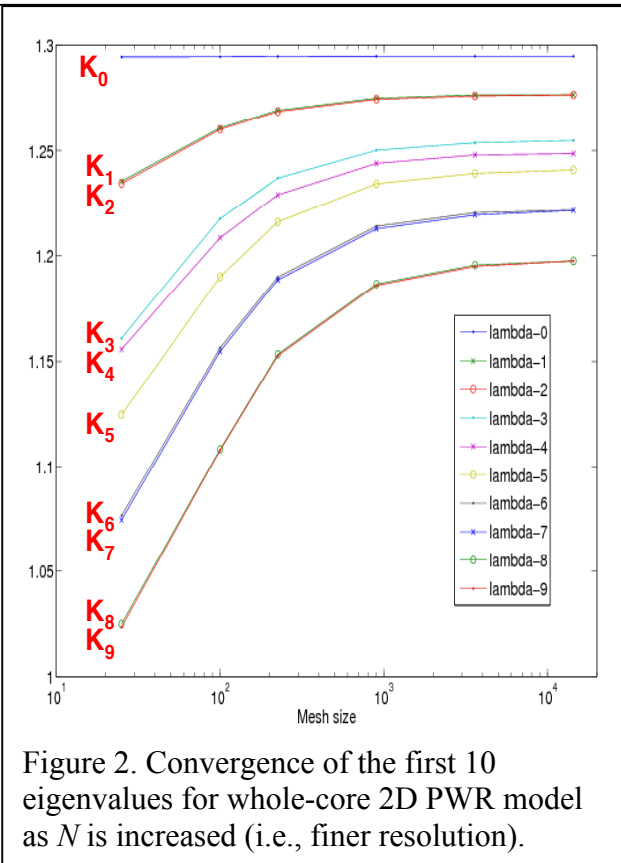
Figure 2 shows the detailed convergence with mesh refinement of the first 10 eigenvalues for this model, indicating that these eigenvalues have converged for  $N = 14,400$  (corresponding to fission matrix dimensions of 14,400 x 14,400).

These mesh refinement studies demonstrate that the eigenvalue spectrum converges smoothly to a stationary discrete distribution. Further mesh refinement will not change the spectrum of lower eigenvalues, indicating that the fission matrix results have converged to the limiting values of the fully-continuous form of the transport equation.



### 4.3 Real vs. Complex Eigenvalues

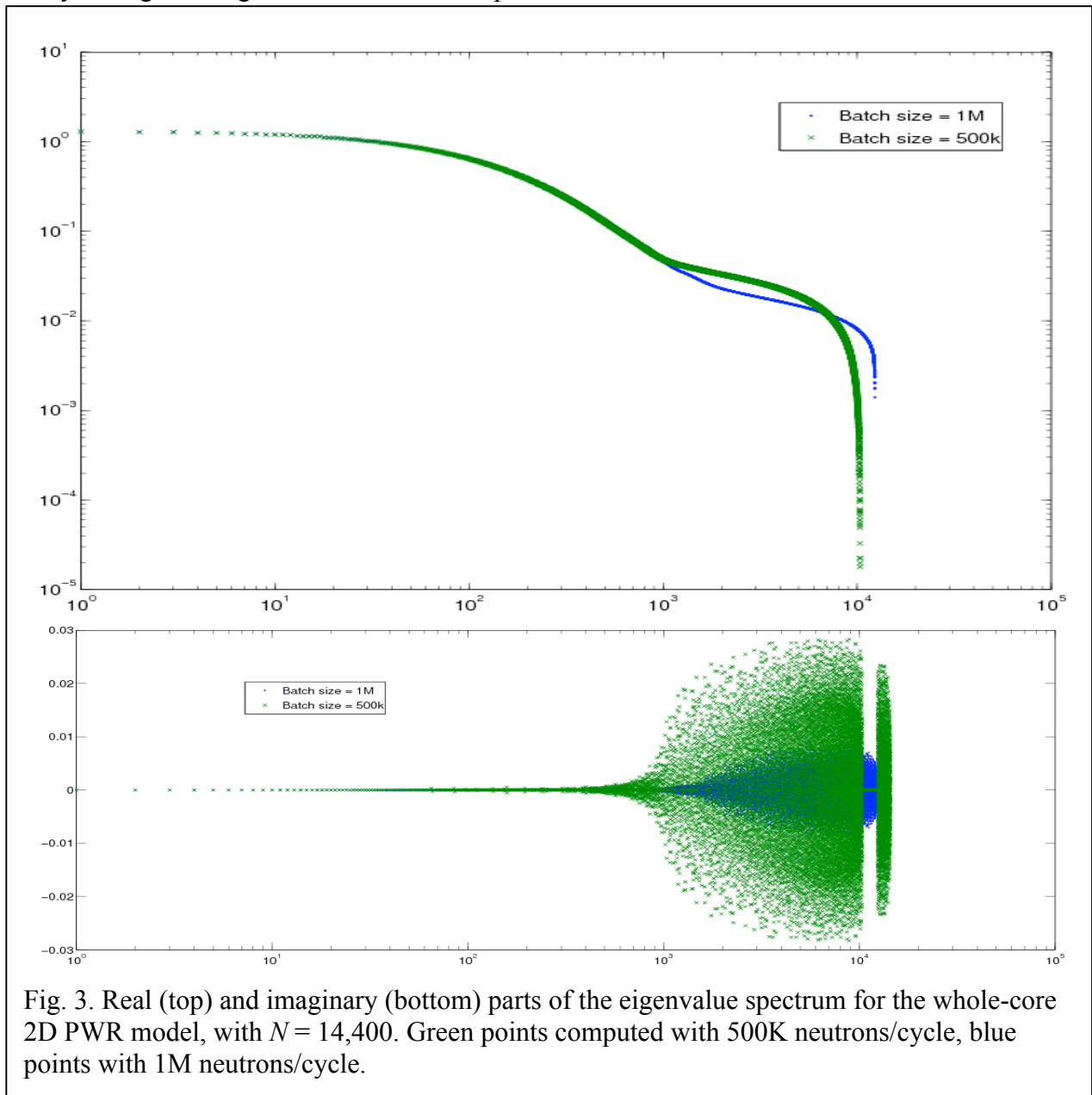
While it has almost always been assumed that the eigenvalues of the transport equation are strictly real, there is no proof of that for continuous-energy problems. Since the fission matrix is nonsymmetric, complex eigenvalues could be present. In the present study, we have also examined this issue. Figure 3 shows the real and imaginary parts of the eigenvalue spectrum for the whole-core 2D PWR model corresponding to Figures 1 and 2. In Fig. 3, the mesh resolution is fixed at  $N = 14,400$ , and the number of neutron histories in the calculations is varied, with the blue points corresponding to twice the number of histories. It is seen that the imaginary portion of the eigenvalues is negligible or zero for the first few hundred eigenvalues. With more neutron histories (blue points in the plots), hence smaller uncertainties in the tallies for the fission matrix elements, the imaginary components become smaller and are shifted to higher portions of the spectrum. It is



speculated that the imaginary portions of the eigenvalue spectrum are artifacts of the statistical noise in the fission matrix elements, and that these artifacts are most apparent for the highest modes. The highest modes are the ones most sensitive to mesh refinement and statistical noise, since the spatial variation of those modes is highly oscillatory and comparable to the mesh region sizes. This evidence is highly suggestive that the eigenvalue spectrum is both discrete and real. Further studies with greater numbers of neutron histories are needed to confirm that speculation.

#### 4.4 Near-Orthogonality of Eigenfunctions

As noted in Section 4.1, the continuous-energy transport equation is biorthogonal, and there is no *a priori* basis for assuming that the forward eigenfunctions form a complete, orthogonal set. Using eigenfunctions determined from the fission matrix method with  $N = 14,400$  for the whole-core 2D PWR model, however, inner products of the lowest eigenfunctions appear to be very nearly orthogonal. Figure 4 shows the inner products for all combinations of the first 25



eigenfunctions (the X-Y axes are the mode numbers). There are only a few off-diagonal terms in the plot, indicating that the forward eigenfunctions are very nearly self-adjoint. Similar analysis for other reactors, including 3D models, also gives similar results for the inner products of the forward modes. It is speculated that this is largely due to the regular and repeating nature of reactor geometry, and is not an inherent property of the underlying continuous-energy transport equation.

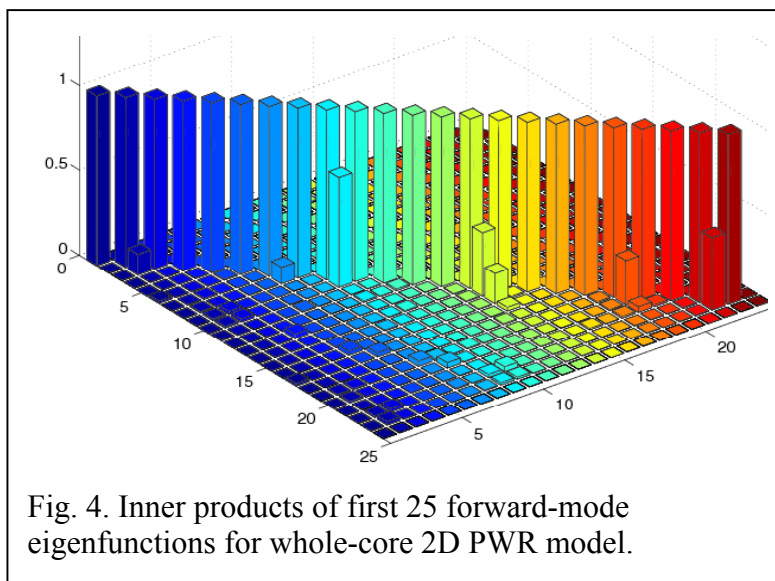


Fig. 4. Inner products of first 25 forward-mode eigenfunctions for whole-core 2D PWR model.

## 5. CONCLUSIONS AND FUTURE WORK

The theory underlying the fission matrix method was derived using a rigorous Green's function approach. The method was then used to investigate fundamental properties of the transport equation for a continuous-energy physics treatment. Numerical evidence from this work suggests that an infinite set of discrete, real eigenvalues and eigenfunctions exist for the continuous-energy problem, and that the eigenvalue spectrum converges smoothly as the spatial mesh for the fission matrix is refined. It was also shown that if the mesh is sufficiently refined so that both forward and adjoint solutions are valid, then the adjoint fission matrix is identical to the transpose of the forward matrix. While the energy-dependent transport equation is strictly biorthogonal, we obtained results that the forward modes are very nearly self-adjoint for a variety of continuous-energy problems. A companion paper (Part II – Applications) describes the initial experience and results from implementing this fission matrix capability into the MCNP Monte Carlo code.

## ACKNOWLEDGMENTS

This work was supported by the US DOE/NNSA Nuclear Criticality Safety Program and by the US DOE/NNSA Advanced Simulation & Computing Program.

## REFERENCES

1. X-5 Monte Carlo Team, “MCNP – A General Monte Carlo N-Particle Transport Code, Version 5, Volume I: Overview and Theory,” LA-UR-03-1987, *Los Alamos National Laboratory* (2003).
2. K.W. Morton, “Criticality Calculations by Monte Carlo Methods”, United Kingdom Atomic Energy Research Establishment, Harwell, Report T/R-1903 (1956).
3. E.L. Kaplan, “Monte Carlo Methods for Equilibrium Solutions in Neutron Multiplication”, Lawrence Radiation Laboratory, UCRL-5275-T (1958).
4. J.M. Hammersely & D.C. Handscomb, Monte Carlo Methods, Chapter 8, Methuen & Co. (1964).
5. S.E. Carney, F.B. Brown, B.C. Kiedrowski, W.R. Martin, Fission Matrix Capability for MCNP, Part II – Applications”, this conference (2013).
6. G.I. Bell & S. Glasstone, Nuclear Reactor Theory, Van Nostrand Reinhold (1970).
7. G. Birkhoff & R.S. Varga, “Reactor Criticality and Nonnegative Matrices”, *J. Soc. Indust. Appl. Math.*, Vol 6, No 4, 354-377 (1958).
8. J. Lehner & G.M. Wing, *Comm. Pure Appl. Math.*, VIII, 217 (1955).
9. D.C. Sahni, “Some New Results Pertaining to Criticality and Time Eigenvalues of One-Speed Neutron Transport Equation”, *Prog. Nuc. Energy*, Vol. 30, No. 3, 305-320 (1996).
10. F.B. Brown, “A Review of Best Practices for Monte Carlo Criticality Calculations”, ANS NCS-2009, Richland, WA, Sept 13-17 (2009).
11. M. Nakagawa & T. Mori, “Whole Core Calculations of Power Reactors by use of Monte Carlo Method”, *J. Nuc. Sci. and Tech.*, **30** [7], pp 692-701 (1993).
12. M.B. Chadwick, et al., “ENDF/B-VII.0: Next Generation Evaluated Nuclear Data Library for Nuclear Science and Technology”, *Nuclear Data Sheets* **107**, 2931–3060 (2006).

## APPENDIX A

Throughout the analysis presented in Sections 2 and 3, it was assumed that the fission neutron emission spectrum  $\chi(E)$  was independent of the incoming neutron energy. This is a usual assumption for the analysis of fast or thermal reactors, but may introduce approximation for intermediate reactors or some critical experiments. In practice, with MCNP and most other Monte Carlo codes,  $\chi(E)$  is indeed a function of the energy of the incident neutron causing the fission. The analysis in Sections 2 and 3 is unchanged, however, if  $\chi(E)$  is replaced by  $\chi(E, \vec{r})$ , defined as the average emission spectrum at position  $\mathbf{r}$ .

$$\chi(E, \vec{r}) = \frac{\iint dE' d\Omega' \chi(E' \rightarrow E) v \Sigma_f(\vec{r}, E') \Psi(\vec{r}, E', \Omega')}{\iint dE' d\Omega' v \Sigma_f(\vec{r}, E') \Psi(\vec{r}, E', \Omega')}$$

This energy-averaged spectrum would need to be tallied consistently with the tallies for the fission matrix elements during the course of the Monte Carlo simulation, but that is rather straightforward. Regarding the analysis in Sections 2 and 3, the use of an average spectrum  $\chi(E, \vec{r})$  introduces an additional approximation, similar to the spatial weighting of the fission matrix elements. It is assumed that with a fine-enough mesh, this approximation would have negligible effect, similar to the discussion regarding Eqs. (33) and (34).